

# **SUPPORTING INFORMATION: “Ultrafast Deactivation of Bilirubin: Dark Intermediates and 2-Photon Isomerization”**

Carlos Carreira Blanco,<sup>†</sup> Patrick Singer,<sup>‡</sup> Rolf Diller,<sup>\*,‡</sup> and J. Luis Pérez  
Lustres<sup>\*,†</sup>

<sup>†</sup>*Centro Singular de Investigación en Química Biolóxica e Materiais Moleculares (CIQUS) and  
Department of Physical Chemistry, Universidade de Santiago de Compostela, C/ Jenaro de la  
Fuente s/n, E-15782 Santiago de Compostela (Spain)*

<sup>‡</sup>*Fachbereich Physik, Technische Universität Kaiserslautern, Erwin Schrödinger Straße, Building  
46, D-67663 Kaiserslautern (Germany)*

E-mail: diller@physik.uni-kl.de; luis.lustres@usc.es

Phone: +34 8818 15722. Fax: +34 8818 15704

## Steady-State Fluorescence Spectroscopy

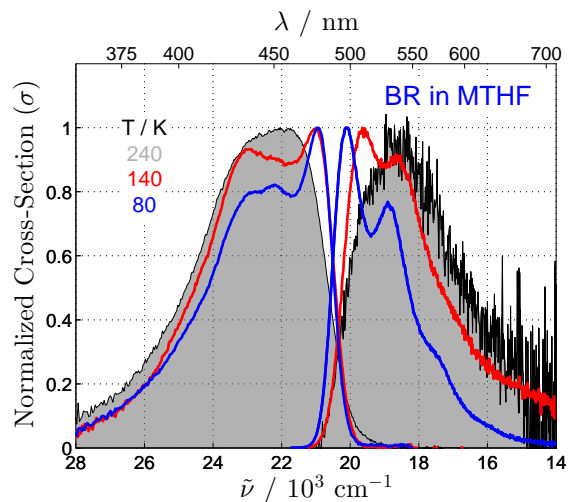


Figure SI 1: Cross-section for absorption (left) and SE (right) of BR in MTHF. The spectra in a MTHF glass at 80 K (blue) are compared with the spectra near the melting point of MTHF (140 K, red) and in the liquid at 240 K (grey-filled).

## Analysis of fs UV-Vis Transient Absorption

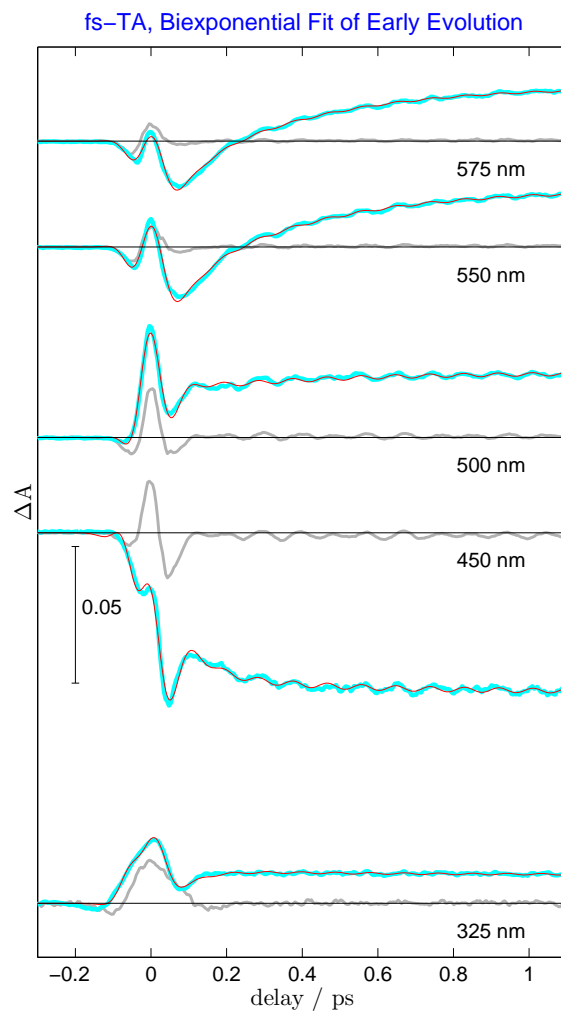


Figure SI 2: fs-TA signal (cyan) of BR in chloroform at the indicated probe wavelengths after 400 nm excitation. The grey line represents the non-resonant solvent signal measured in the same experimental conditions. The red line shows the data fit with two exponential functions, an offset and a damped oscillation. Signal amplitude is given by the inner gauge.

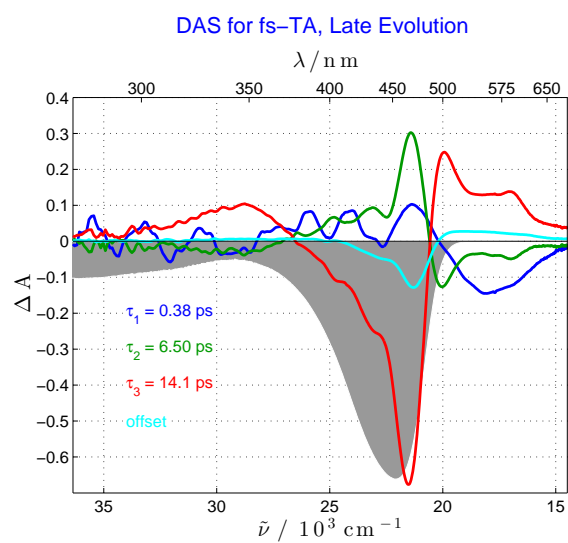


Figure SI 3: Decay associated spectra (DAS) deduced from the triexponential fit of fs-TA data in the 100 ps timescale. Decay times of 0.38, 6.50 and 14.1 ps were deduced. Their DAS are indicated by the colour of the specific legend. The spectrum of the long living component is shown in cyan.

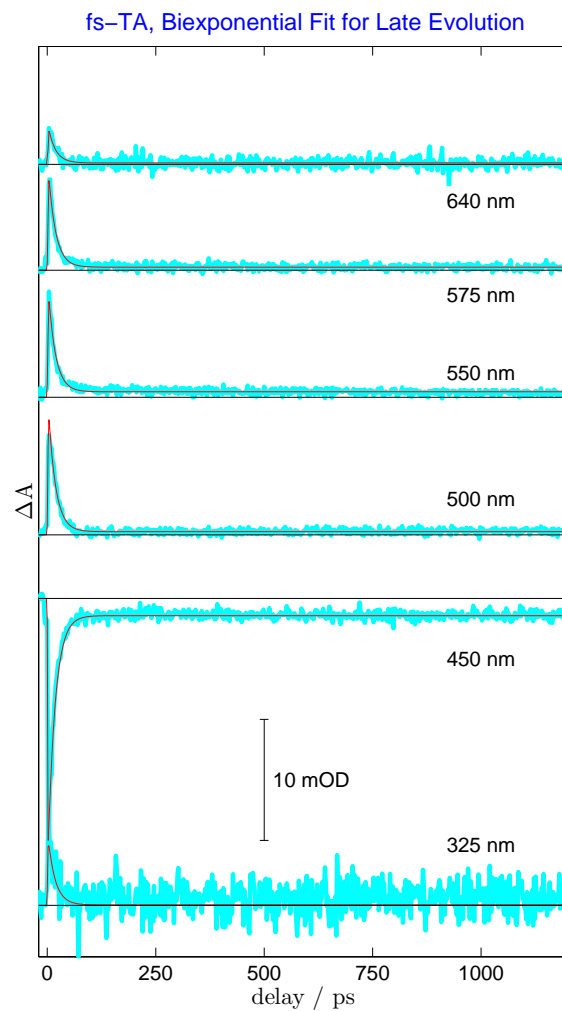


Figure SI 4: fs-TA signal (cyan) of BR in chloroform at the indicated probe wavelengths after 400 nm excitation. The pump energy was  $0.6 \mu\text{J}$  in this experiment. The red line shows the fit with two exponential functions and an offset. Signal amplitude is given by the inner gauge.

BR/CHCl<sub>3</sub>, photoequilibrium spectra from Lightner et al.

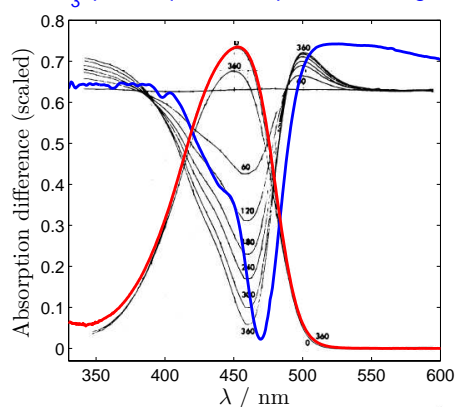


Figure SI 5: Non-decaying component (blue) observed by us after ultrafast excitation of BR at 400 nm. The pump energy was 0.9  $\mu\text{J}$  for this experiment. The linear absorption band-shape of BR in the ground state is shown in red. The background shows “the absorption difference spectra obtained from irradiation of 15  $\mu\text{M}$  BR solutions” in chloroform with 1% ethanol, as published by Lightner *et al.* in the Figure 1 of Reference 1. The cumulative irradiation time is indicated in seconds. The authors assigned the spectral evolution upon steady-state irradiation to a shift in the photo-equilibrium  $(4Z, 15Z) \rightleftharpoons (4Z, 15E) + (4E, 15Z)$ . The 4E,15Z geometrical isomer would form in minor amounts.

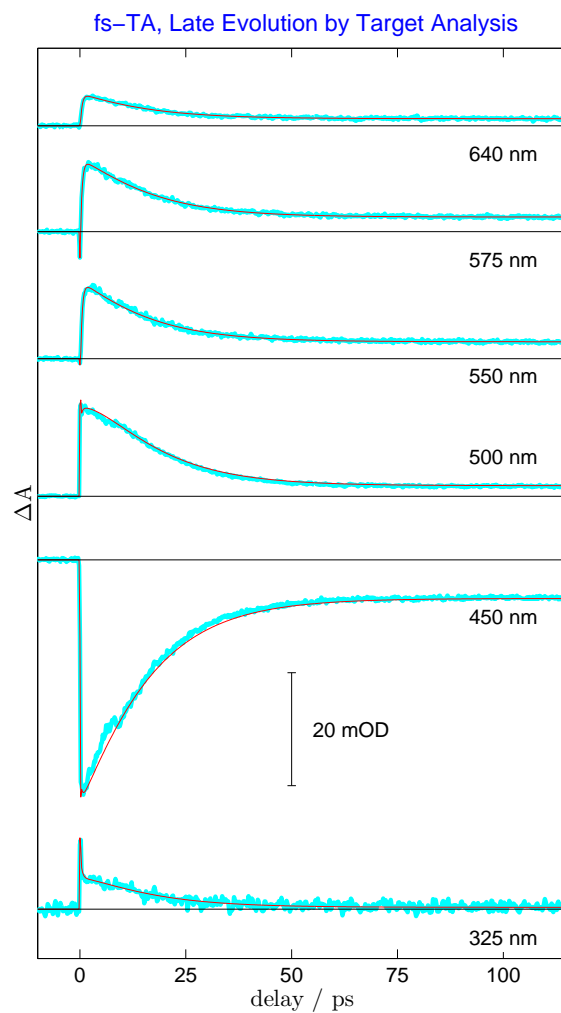


Figure SI 6: fs-TA signal (cyan) of BR in chloroform at the indicated probe wavelengths after 400 nm excitation. The pump energy was 0.9  $\mu\text{J}$  in this experiment. The red line shows the fit with the time-dependent concentrations deduced from the mechanism in the Scheme 2. Signal amplitude is given by the inner gauge.

## Transient Absorption Anisotropy

The fs transient absorption anisotropy ( $r$ ) was obtained from independent measurements done with parallel ( $\Delta A_{\parallel}$ ) and perpendicular ( $\Delta A_{\perp}$ ) pump-probe polarizations and according to the definition  $r = \frac{\Delta A_{\parallel} - \Delta A_{\perp}}{\Delta A_{\parallel} + 2\Delta A_{\perp}}$ . The anisotropy spectrum can be determined accurately in the spectral window extending from 420 to 640 nm at early delays, Figure SI 7. The gap around 490 nm results from the zero amplitude of the signal at this wavelength. The anisotropy spectrum remains roughly constant between 450 and 480 nm and between 510 and 550 nm, so that signal averaging in both spectral windows is justified. The so-obtained time-dependent anisotropy signals are shown in Figure SI 8. The signal evolves mainly on the time scale of 200 ps and appears to show minor evolution in the nanosecond time window. Essentially the same behaviour is observed in the bleach and ESA regions. Note however that the one-photon contribution has already decayed to less than 90% of the time-zero amplitude at 50 ps delay (Figure 2), which means that the parallel and perpendicular signals are very close to zero at late delays, typically few mOD. This translates into a substantial error of the anisotropy at delays longer than 50 ps, where the two-photon processes further complicate signal analysis. This could be the reason why the anisotropy traces in Figure SI 8 tend asymptotically  $\approx -0.15$  instead of zero, as expected for the isotropic orientation of transition dipoles. Therefore, we conclude that the time-evolution of the anisotropy suggests that rotational diffusion of BR occurs with a characteristic time constant of 100-200 ps. Significant uncertainties in our transient anisotropy signal at late delays hinder a deeper analysis of BR rotational diffusion.

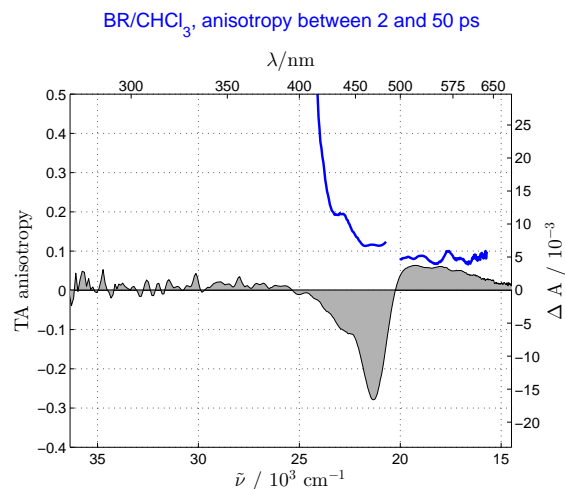


Figure SI 7: Anisotropy of the fs-TA signal of BR in chloroform (blue, left axis) time-averaged between 2 and 50 ps pump-probe delays with 400 nm excitation. The pump energy was 0.9  $\mu\text{J}$  in this experiment. The grey-filled curve shows the transient spectrum at 50 ps delay (right axis).

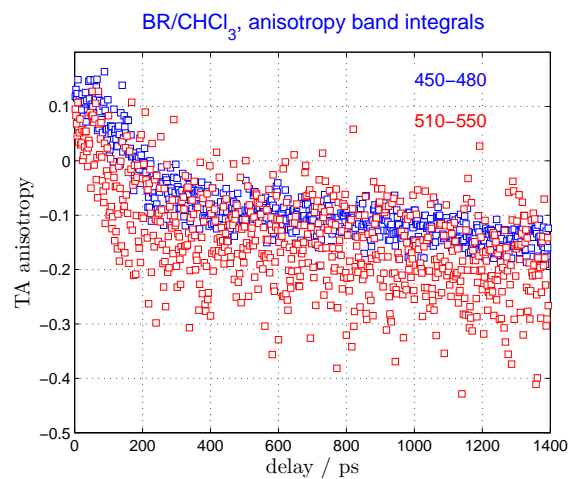


Figure SI 8: Band integrals of the anisotropy TA signal of BR in chloroform with 400 nm excitation. The signal anisotropy was obtained through independent measurements at parallel and perpendicular pump-probe polarizations. The band integrals were calculated between 450 and 480 nm (blue squares) and between 510 and 550 nm (red squares), where the anisotropy spectrum is constant within experimental accuracy. The pump energy was 0.9  $\mu\text{J}$  in this experiment.

## Analysis of fs mid-IR Transient Absorption

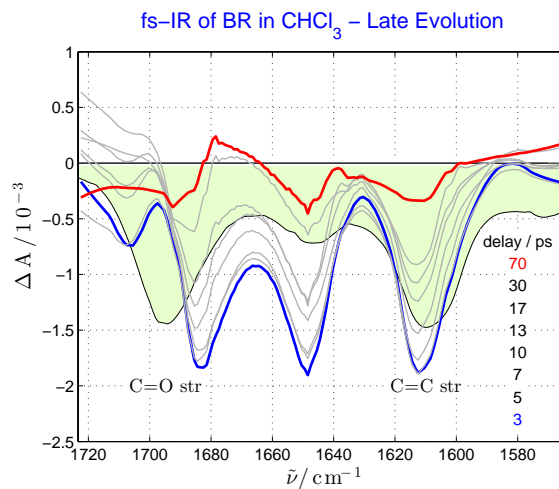


Figure SI 9: Vis-pump/mid-IR probe transient absorption spectra of BR in chloroform at the indicated pump-probe delays in the C=C and C=O *str* regions. The steady-state mid-IR absorption spectrum is shown as a light-green-filled curve. Transient spectra were measured in three independent windows (1580-1635, 1610-1680 and 1650-1730  $\text{cm}^{-1}$ ), joined and smoothed with a Savitzki-Golay filter for better visibility. Late spectral evolution is shown.

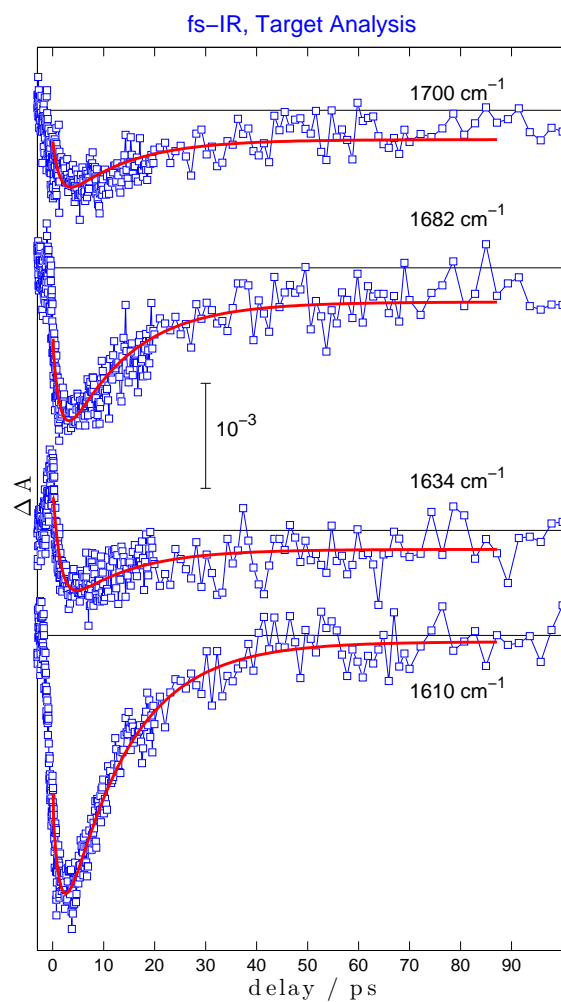


Figure SI 10: Global target analysis (red) of the fs transient absorption signal (blue squares) of BR in chloroform at the indicated frequencies and after 490 nm excitation. A non decaying component is also included in the fitting function but the associated amplitude is the range of the background noise so that no conclusion can be drawn about non-decaying species. The signal amplitude is given by the inner gauge.

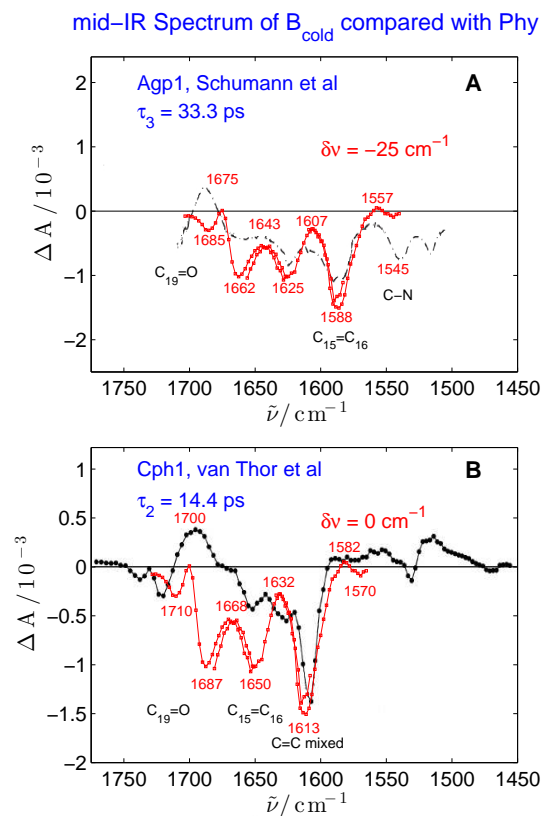


Figure SI 11: mid-IR SAS of the  $B_{cold}$  species (red) compared with the DAS of the 33.3 ps component observed for the decay of the bilin chromophore in the Agp1 phytochrome (Phy) from *Agrobacterium tumefaciens*<sup>2</sup> (black, panel A) and for the 14.4 ps component in the Cph1 Phy from *Cyanobacterium synecocystis* PCC 6803<sup>3</sup> (black, panel B). The  $B_{cold}$  spectrum was down-shifted by 25 cm<sup>-1</sup> in panel A only. The band assignments done in each publication are shown as inset, labels are located at the exact positions of the assignments in the ground state of the bilin chromophore in each protein. The peak positions for the spectra in our work are shown in red.

## Time Dependent Concentrations

The one-photon mechanism is shown as inset in Figure 3. The deduced time-dependent concentrations are collected in Equations SI.1, where  $a_0$  is the time-zero concentration placed by the excitation pulse in state **A** and  $c_0^{2Ph}$  is the time-zero concentration brought to a high excited state by two-photon excitation. In the one-photon process, **A** relaxes to **B** with a rate constant  $k_1$ . We note that the wavepacket propagates in the Franck-Condon potential well with a rate constant of 0.06 ps but this process goes unnoticed at long delays and is not included in the mechanism for the sake of conciseness. **B** further relaxes with a rate constant  $k_2$  to **B<sub>cold</sub>** and the latter decays to the ground state with the rate constant  $k_B$ . **C** is assumed to form impulsively from the high excited state after two-photon excitation. One-photon excitation is also expected to produce **C** but with much lower yield.<sup>1,4-6</sup> Thus, the signal of **C** measured with parallel pump-probe polarization appears to decay by rotational diffusion with a rate constant  $k_{RD}$ . It is deduced that the spectrum measured at long delay times corresponds only to **C**, precursor of the (4Z,15E) isomer.

$$\begin{aligned}
 [A](t) &= a_0 \times e^{-k_1 t} \\
 [B](t) &= \frac{a_0 k_1}{k_2 - k_1} \times \{e^{-k_1 t} - e^{-k_2 t}\} \\
 [B_{cold}](t) &= \frac{a_0 k_1 k_2}{(k_2 - k_1)(k_1 - k_B)(k_2 - k_B)} \times \\
 &\quad \{-(k_2 - k_B)e^{-k_1 t} + (k_1 - k_B)e^{-k_2 t} + (k_2 - k_1)e^{-k_B t}\} \\
 [C](t) &= c_0^{2Ph} (1 - e^{-k_{RD} t})
 \end{aligned} \tag{SI.1}$$

The above discussed mechanism has to be adapted to the lower time resolution of the mid-IR experiment. Thus,  $k_1$  is close to the resolution limit if one considers the broader cross-correlation and the weaker signal-to-noise in the mid-IR, where the transient signal reaches maximum values of  $2 \times 10^{-3}$ . Our best fit resolves an average time constant of 1.5 ps resulting from  $k_1$  and  $k_2$  together. Thus, earliest mid-IR spectra represent a time average over the **A** and **B** SAS which give rise to **B<sub>cold</sub>**. The later decays via  $k_B$ . No long-living species could be detected faithfully in the mid-IR.

Therefore, we use the time-dependent concentrations in Equations SI.2 for the mid-IR experiment.

$$\begin{aligned} [AB](t) &= a_0 \times e^{-\bar{k}_{12}t} \\ [B_{cold}](t) &= \frac{a_0 \bar{k}_{12}}{k_B - \bar{k}_{12}} \times \{e^{-\bar{k}_{12}t} - e^{-k_B t}\} \end{aligned} \quad (\text{SI.2})$$

## Experimental Part

### Sample Preparation and Materials

Bilirubin (BR) was purchased from Acros Organics (99%) and used as received. Solutions were freshly prepared in spectroscopic grade non-degassed solvents from Aldrich, Fischer, Scharlau and Merck. The concentration was kept below  $10^{-5}$  M in fluorescence measurements, so that spontaneous fluorescence and absorption spectra can be accurately measured for the same sample without inner filter effects. For low-temperature measurements, samples were dissolved in 2-methyltetrahydrofuran (MTHF) and degassed by the freeze-pump-thaw technique with a turbo-molecular pump (Balzers, four cycles,  $\approx 10^{-5}$  mbar) in a fused silica cuvette. Clear organic glasses were prepared by slow freezing of the MTHF solutions down to 80 K. Highly concentrated samples were used for fs measurements, absorption was typically 0.6 at 450 nm in a 0.3 mm cuvette.

### Absorption and Fluorescence Spectroscopy

Steady-state UV–Vis absorption spectra were scanned in a Varian Cary 3E double-beam spectrophotometer. Fluorescence spectra were acquired in an Spex Fluorolog 2 spectrofluorometer at right angle geometry. Both kinds of spectra were corrected for the baseline of the solvent. Fluorescence excitation and emission spectra were measured three times and averaged. The spectra were corrected for instrumental factors by multiplying by correction functions obtained by the method of Gardecki and Maroncelli<sup>7</sup> and transformed into cross-sections of stimulated emission for comparison with absorption.<sup>8</sup> All steady-state absorption and fluorescence measurements were done

in 1 cm-thick fused-silica cuvettes and slit widths were chosen so that acceptable signal-to-noise ratios were reached: 2 nm of absorption and 1 – 2 nm for fluorescence. The samples were brought into an Oxford Instruments DN 1704 liquid nitrogen cryostat for low temperature measurements.

## **IR Spectroscopy**

IR spectra were measured in a Nicolet 380 FT-IR (Thermo Electron Co) spectrometer by ATR and transmission (0.25 mm cell) in the 400 – 4000  $\text{cm}^{-1}$  spectral window with  $\approx 1 \text{ cm}^{-1}$  resolution. 300 scans were averaged and corrected for the background of solvent and cell.

## **Femtosecond Optical Spectroscopy**

The femtosecond transient absorption setup at the University of Santiago was analogous to the one described in References 9 and 10. Briefly, basic pulses were delivered by a multipass Ti:Sa amplifier (Femtolasers Femtopower Compact Pro, 30 fs pulses centred at 800 nm and with 0.8 mJ energy at 720 Hz). A part of the fundamental beam was frequency doubled in a 0.2 mm BBO crystal (Eksma) and compressed with a prism pair. The 400 nm pulses were further divided for optical excitation (0.3-1.7  $\mu\text{J}$ ) and for white-light continuum generation in a  $\text{CaF}_2$  plate (5  $\mu\text{J}$ ). The continuum was filtered and split for reference before being imaged onto the sample cell (spot size  $\approx 100 \mu\text{m}$ , flow-rate 1  $\mu\text{l}$  per excitation pulse, 0.2 mm window thickness and 0.3 mm cell thickness). Transmitted and reference beams were further imaged onto the entrance planes of separate home-made flat-field spectrographs and registered by photodiode arrays with 512 pixels (Hamamatsu S3901-512Q). The spectral resolution is below 2 nm. Measurements were performed at parallel and perpendicular polarizations and one transient spectrum represents the average of 100 consecutive shots. Transient spectra were acquired with constant step-size. Step-sizes ranging from 5 fs to 2 ps were employed and four to eight independent scans were averaged. Pump-probe cross-correlation was estimated by the non-resonant coherent solvent signal. The average cross-correlation FWHM was found to be 90 fs across the full spectral window, being shorter around 400 nm and deteriorating in the UV. Transient spectra were corrected for the chirp of the

continuum. fs-TA measurements were performed in chloroform.

## Femtosecond Vis Pump–mid-IR Probe Spectroscopy

The fs Vis pump–mid-IR probe setup was also described elsewhere.<sup>11</sup> Briefly, fundamental pulses were derived from a CPA 2001 (Clark-MXR) regenerative Ti:Sa laser system. It pumps a home-built two-stage NOPA tuned in the visible and a two-stage OPA coupled to a AgGaS<sub>2</sub> stage for difference frequency generation in the mid-IR. 400 nJ, 50 fs pump pulses centred at 490 nm were focused to a spot size of 150  $\mu\text{m}$  in a 2 mm CaF<sub>2</sub> cuvette and used as Vis pump. Mid-IR pulses with a typical width of 100  $\text{cm}^{-1}$  were used as probe. The mid-IR chamber was purged with dry air to avoid pulse lengthening and IR absorption by water. Measurements were performed in three spectral windows centred at 1600, 1645 and 1690  $\text{cm}^{-1}$ . The resulting Vis pump–mid-IR probe cross-correlation measured in a thin Silicon wafer is about 400 fs, although time fits indicate that the cross-correlation is about two times shorter. The transient signal is dispersed in a TRIAX 320 polychromator with a linear dispersion of 19.7 nm/mm (Jobin Yvon) and imaged onto a 32-element HgCdTe array cooled by liquid N<sub>2</sub>. The spectral resolution is typically 2.5  $\text{cm}^{-1}$ .

## References

- (1) Lightner, D. A.; Wooldridge, T. A.; McDonagh, A. F. *Proc. Natl. Acad. Sci. U.S.A.* **1979**, *76*, 29–32.
- (2) Schumann, C.; Gross, R.; Michael, N.; Lamparter, T.; Dilier, R. *Chemphyschem* **2007**, *8*, 1657–1663.
- (3) van Thor, J. J.; Ronayne, L.; Towrie, M. *J. Am. Chem. Soc.* **2007**, *129*, 126–132.
- (4) Migliorini, M. G.; Galvan, P.; Sbrana, G.; Donzelli, G. P.; Vecchi, C. *Biochem. J.* **1988**, *256*, 841–846.
- (5) McDonagh, A. F.; Agati, G.; Lightner, D. A. *Monatsh. Chem.* **1998**, *129*, 649–660.

- (6) Mazzoni, M.; Agati, G.; Troup, G. J.; Pratesi, R. *J. Opt. A: Pure Appl. Opt.* **2003**, *5*, 374–380.
- (7) Gardecki, J. A.; Maroncelli, M. *Appl. Spectrosc.* **1998**, *52*, 1179–1189.
- (8) Birks, J. B. *Photophysics of Aromatic Molecules*; Wiley Monographs in Chemical Physics; Wiley-Interscience, 1970.
- (9) Dobryakov, A. L.; Kovalenko, S. A.; Weigel, A.; Perez-Lustres, J. L.; Lange, J.; Mueller, A.; Ernsting, N. P. *Rev. Sci. Instrum.* **2010**, *81*, 113106.
- (10) Kovalenko, S. A.; Dobryakov, A. L.; Ruthmann, J.; Ernsting, N. P. *Phys. Rev. A* **1999**, *59*, 2369–2384.
- (11) Peters, F.; Herbst, J.; Tittor, J.; Oesterhelt, D.; Diller, R. *Chem. Phys.* **2006**, *323*, 109–116.